

Chapter 2

How to Measure Heat Capacity at Low Temperatures

Abstract This chapter is devoted to the description of calorimetric techniques used to measure heat capacity of solids: pulse heat calorimetry (Sect. 2.3), relaxation calorimetry (Sect. 2.4), dual slope calorimetry (Sect. 2.5), a.c. calorimetry (Sect. 2.6), differential scanning calorimetry (Sect. 2.7). Examples of measurements of heat capacity are reported in Sects. 2.3 and 2.4.

2.1 Introduction

Specific heat defined by (1.4) is useful only if the material is homogeneous. In this chapter, the heat capacity of the sample under measurement will always be considered in order to also include data about inhomogeneous devices of cryogenic interest (see, e.g., Ref. [1]).

When a power, $P(t)$, is supplied to an isothermal sample of heat capacity $C_S(T)$ in adiabatic conditions, the sample heating is described by

$$P(t)dt = C_S(T)dT. \quad (2.1)$$

If the initial temperature (at $t = t_0$) of the sample is T_0 , at the time t , the sample temperature will be found by integration of (2.1)

$$\int_{t_0}^t P(t)dt = Q = \int_{T_0}^T C_S(T)dT \quad (2.2)$$

where Q is the total heat supplied to the sample in the time interval $(t - t_0)$.

Equation (2.2) finds two basic applications:

- (a) Evaluation of Q if $C_S(T)$ is known and T is measured (detectors)
- (b) Evaluation of $C_S(T)$ if both Q and T are measured.

We are interested in the second application. The apparatus which measure $C_S(T)$ at any temperature is called the “calorimeter”.

To measure the heat capacity of a sample at low temperature, we must refrigerate the material of mass m to the starting temperature T_0 , isolate it thermally from its environment (for example, by opening a heat switch, [2] and supply an amount of heat Q to reach the final temperature T . The result is often shown in the form $C_S = Q/(T - T_0)$ at the intermediate temperature $T_i = (T + T_0)/2$.

In most cases, a low temperature calorimeter is fabricated following the scheme of Fig. 2.1. It usually consists of a platform (the sample holder) to which a sample of heat capacity C_S , a thermometer T_{SH} , and a heater H are mechanically and thermally connected often by glue or vacuum grease. A thermal resistance R_{Tb} links the platform to the thermal bath, while R_{SH} is the thermal resistance between the sample and the sample holder. Depending on the shape and size of the sample and on the used experimental method, the thermometer and the heater can be connected to the sample holder as indicated in Fig. 1.22 or can be directly glued on the sample. In both cases, a good thermal contact between the sample and the thermometer has to be reached. If the product $R_{SH}C_S$ is much smaller than $R_{Tb}C_{SH}$ (neglecting the time constants associated to heater and thermometer), the temperature of the sample T_S is equal to T_{SH} during the measurement. The thermal contact resistance between the thermometer and the sample holder, and between the heater and the sample holder are labeled as R_{CT} and R_{CH} , respectively.

As we shall see in Sect. 2.2, a basic distinction can be made between an adiabatic ($R_{Tb} = \infty$) and nonadiabatic ($R_{Tb} \neq \infty$) situation. The former condition can only be approximated: no calorimeter is perfectly adiabatic. The more traditional adiabatic methods are based on a good thermal isolation of the sample, and the use of a heat switch to connect and disconnect the calorimeter to the bath. However, heat switching may give rise to experimental problems since, especially with small samples at very low temperatures, the influence of parasitic heat leaks may become dominant. Therefore, scientists have developed several techniques in which there is no need of a complete thermal isolation, and in which the sample is linked to a heat sink by a thermal conductance $R_{Tb} \neq \infty$.

In general, the heat capacities of the addenda (sample holder, thermometer, glues, leads) are small compared to that of the sample; otherwise, addenda heat capacities have to be known with sufficient accuracy from an additional measurement without a sample, or evaluated by the exact knowledge of their mass and specific heats (for subtracting it from the total measured value). The leads to the thermometer and heater must be of low thermal conductance (for measurements at $T \ll T_C$, the best are thin superconducting wires) and have to be carefully heat-sunk at a temperature close to the temperature of the sample to avoid heat flow into it. The heat capacities of wires contribute to the addendum [3]. The thermometer, heater and the sample should, of course, be thermally well-coupled to the platform in order to avoid unknown temperature differences. The power supplied to the thermometer should be small enough to avoid overheating [2]. Parasitic heat losses or heat inflow by radiation must be reduced by a thermal shield at a temperature very close to the temperature of the sample. When a heat switch is present, heat

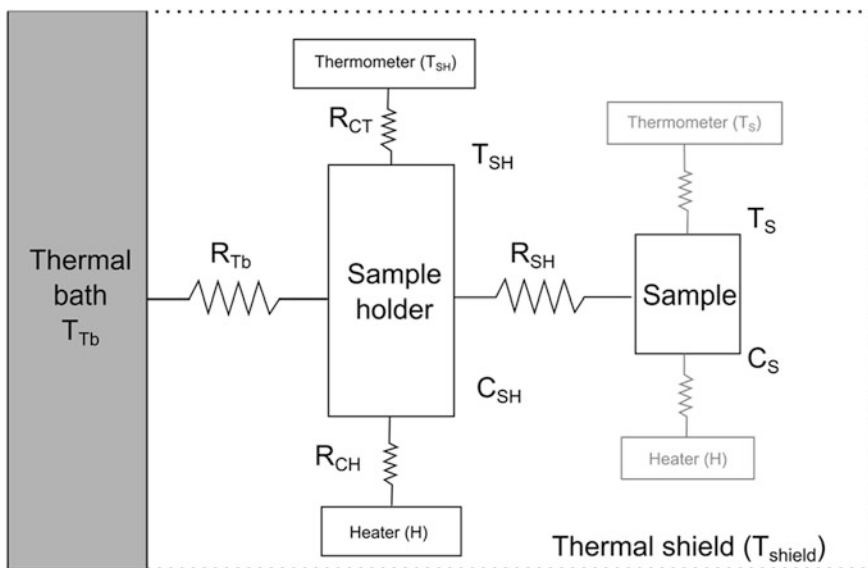


Fig. 2.1 Scheme of the main elements of a calorimeter for measurements of heat capacity

produced by opening and/or closing should be small. If an exchange gas is used to cool down the calorimeter, it has to be carefully pumped away before carrying out the measurement. Also, the possibility of adsorption and desorption of residual gas when the temperature is changed should be taken into account since it involves heat of adsorption/desorption.

As a result of these problems, heat-capacity data rarely have accuracy better than 1 %, though more often it is 3–5 %. If high accuracy is needed or the parameters of the setup are not well known, the calorimeter accuracy can be validated by measuring the heat capacity of a well-known reference sample [4–9].

Continuous improvements in calorimetry have been achieved due to advances in electronics, thermometers, microfabrication techniques, and computer automation. In particular, one has to keep in mind that the accuracy of the thermometer is a critical parameter in this type of measurement.

2.2 Calorimeters

Calorimetry started in the 18th century with the pioneering studies of Joseph Black [10] who first introduced the concepts of latent heat and heat capacity. The term calorimeter is used for the description of an instrument devised to determine heat and the rate of heat exchange or, *vice versa*, heat capacity if the first two quantities are measured, following (2.2).

The design of calorimeters has been modified and adapted for plenty of purposes, e.g., microcalorimeters and nanocalorimeters are intended to designate calorimeters in which heat capacities of the order of $\mu\text{J/K}$ and nJ/K , respectively, can be detected (see Sect. 2.10). These instruments prompted the study of thermal properties of layers of molecules (generally in the gas phase) adsorbed on a surface.

Depending on the heat transfer conditions between the sample holder and the thermal bath, calorimeters can be classified by isothermal, isoperibol, and adiabatic types. A possible classification and standard nomenclature of calorimeters is reported in [11, 12].

Isothermal calorimeters have both calorimeter and thermal bath at constant T_{Tb} . If the surroundings are only isothermal, the mode of operation is called isoperibol [13]. In adiabatic calorimeters, the exchange of heat between the calorimeter and the shield is kept close to zero by making the thermal conductance as small as possible. Nevertheless, the thermal insulation of the device can never be perfect as long as there is a temperature difference between calorimeter and shield. If the temperature of the shield changes following the temperature of the internally heated calorimeter, there will be no heat flux by radiation or conduction along the supporting elements. This heat compensation becomes particularly important above 100 K, when the radiation heat transfer becomes relevant. The first adiabatic calorimeter was described in 1911 by Nernst [14], who recognized the necessity of thermal insulation for low temperature measurements. Adiabatic conditions become more and more difficult to be fulfilled when the temperature and dimensions of the sample decrease. Semiadiabatic conditions are typically met for samples with masses between 10 mg and 1 g [15]. Nonadiabatic or isoperibol conditions exist when the measured heat capacities are so small that the thermal conductance along the electrical leads cause the sample temperature to decay exponentially towards the shield temperature.

The use of a sample holder, an external thermometer and an electric heater is a common feature of these methods. This kind of setup requires the knowledge of addendum heat capacity, and thus the accuracy of the measurements is limited by the calibration errors.

Within the three groups, several techniques have been used which often mimic the methods used to measure the electrical capacitance according to the equivalence Table 2.1.

Table 2.1 must be used with great caution. In fact, it is possible to use the standard Kirchhoff laws to describe the thermal systems and to solve circuit equations for $T(t)$ or $P(t)$; however, the thermal quantities, such as the thermal resistance and the heat capacity, often have properties that rapidly change with temperature, whereas the electrical quantities, such as capacitance and electrical resistance, are usually almost independent on the voltage. It is worth pointing out that there is no correspondence between the electrical inductance L and the kinetic inductance L_k [16].

The well-known techniques used to solve electric circuit problems can only be employed for “small signals” (see, e.g., [2]). Note that also the equivalence between thermal grounding and electrical grounding only holds for small signals.

Table 2.1 Equivalence between some electrical and thermal parameters

Thermal parameter	Electrical parameter
V (voltage)	T (temperature)
P (power)	I (current)
R (thermal resistance)	R (electrical resistance)
C (heat capacity)	C (capacitance)
Thermal grounding	Electrical grounding

Moreover, the approximation with “lumped elements,” which is an excellent approximation in electrical circuits at low frequency, fails or is a rough approximation in “thermal circuits” even if the latter only involves a frequency range of a few Hz.

Finally, the thermal bath temperature, which is formally equivalent to the electrical ground, is kept at temperature T_{Tb} with fluctuations larger than those of electric V or I supply. Special care should be devoted to the problem of the temperature stability of the bath since the refrigerator has a finite cooling power, and the thermal bath represents a ground (to a good approximation) only in the case that the incoming power on it does not substantially change its temperature.

In analogy with the electrical $I(t)$, the waveform of $P(t)$ appearing in (2.2) is not restricted to sinusoidal oscillations, but can have any other waveform, e.g., impulsive, rectangular or triangular waveforms have been used [17–19]. The modulation was also indirectly induced to the sample by giving a modulated power to the heat shield [20].

Since the pioneering work of Eucken [21] and Nernst [22] in the early 20th century, adiabatic calorimetry has provided the most accurate means of obtaining specific heat data. The high accuracy arises from the simplicity of the measurement principle. The adiabatic measurement approach directly comes from the definition of heat capacity:

$$C_p = \lim_{\Delta T \rightarrow 0} \left(\frac{\Delta Q}{\Delta T} \right)_p. \quad (2.3)$$

Due to the general applicability independent of the sample thermal conductivity, this method is the most favored choice for heat capacity measurements of condensable gases which have poor thermal conductivity in their low temperature solid phase [23–25].

Adiabatic calorimetry is a very precise technique and can be used to determine the latent heat at strong first order transitions. However, it usually lacks in achieving the resolution needed to characterize the temperature dependence of $C_p(T)$ close to the critical temperature T_c for a second-order transition. Also, because of the inherent limitations on getting the ideal adiabatic conditions and the long time required to cover a few tens of K range with reasonable number of data points, nonadiabatic techniques (e.g., the AC calorimetry) are often preferred at low temperatures.

Because of the large quantity of the existing calorimetric methods for the measurements of the heat capacity, we only selected some of them, describing the experimental setup and giving some examples of their applications:

- Heat pulse calorimetry (Sect. 2.3)
- Relaxation calorimetry (Sect. 2.4)
- Dual slope calorimetry (Sect. 2.5)
- AC calorimetry (Sect. 2.6)
- Differential scanning calorimetry (Sect. 2.7).

2.3 Heat Pulse Calorimetry

In the heat pulse technique, we can either be in an adiabatic or nonadiabatic situation. In the former case, (2.3) is applied; in the latter case, the sample is usually connected to the bath through a weak thermal link. Following a heat pulse of energy ΔQ , which is commonly supplied by an electrical heater, the temperature of the sample first rises and then decays to its initial value with a time constant $\tau = R_{Tb}C$, where R_{Tb} is the thermal resistance of the link and C is the total heat capacity of the sample plus addenda ($C = C_S + C_{SH} + C_{add}$). The heat capacity is obtained through $C = \Delta Q/\Delta T$ where ΔT is a suitable extrapolation of the temperature step (see Fig. 2.2). Note that τ should not be too small, even at the lowest temperatures ($\tau \geq 1$ s, in most cases) because of the time response of measuring instruments. The $\Delta T(t)$ curve after a heat pulse has the shape shown in Fig. 2.2. The temperature difference ΔT is also obtained by extrapolating the log plot of the $\Delta T(t)$ curve to the zero time (the time of the end of the heat pulse). Heat pulse calorimetry has been used, e.g., in measurements reported in [26–32].

2.3.1 Example 1: Heat Pulse Calorimeter for a Small Sample at Temperatures Below 3 K

As a typical example of the heat pulse method, we will describe the measurement of the specific heat of Cu and amorphous $\text{Zr}_{65}\text{Cu}_{35}$ reported in [33]. Figure 2.3 shows the experimental setup for the measurement of heat capacity: the sample is glued onto a thin Si support slab. The thermometer is a doped silicon chip and the heater is made by a gold deposition pattern (~ 60 nm thickness) on the Si slab. Electrical wiring to the connecting terminals are made of superconductor (NbTi). The thermal conductance to the thermal bath (i.e., mixing chamber of a dilution refrigerator) is due to four thin nylon threads. The silicon slab, the thermometer and the heater represent the “addendum” whose heat capacity $C_A(T)$ must be measured in a preliminary run.

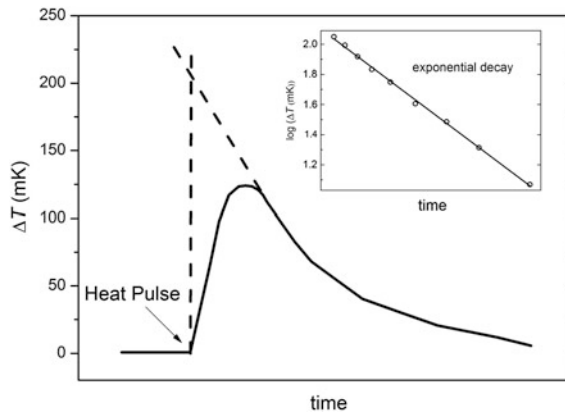


Fig. 2.2 Typical $\Delta T(t)$ curve. The *inset* shows the linear fit applied to the exponential decay after the peak

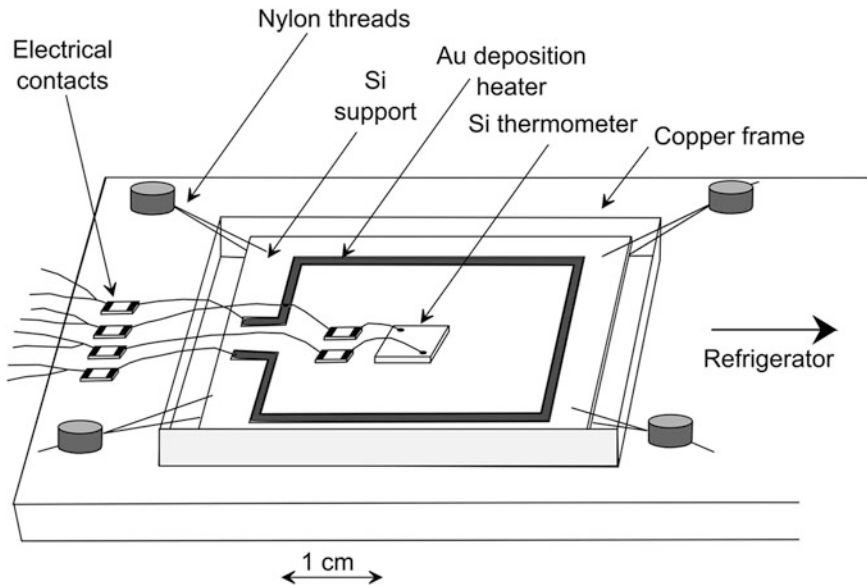


Fig. 2.3 Sample holder for the measurement of heat capacity [33]

When a sample of heat capacity $C(T)$ is added, a second run of measurements gives $C_A(T) + C(T)$. It is obvious that, if possible, the condition $C_A \ll C$ should be fulfilled. For the heat pulse technique, the sample is thermally connected to the cold source through a weak link. Following a heat pulse of energy Q , which is delivered by means of the electrical heater, the temperature of the sample first rises and then decays to its initial value with a time constant $\tau = R_L C_T$. Here, R_L is the

thermal resistance of the link and C_T is the total heat capacity of the sample and addenda (sample holder, heater, thermometer, etc.). C_T is obtained through $C_T = \Delta Q / \Delta T$ where ΔT is a suitable extrapolation of the temperature step.

In this experimental setup, the nylon threads fixing the sample holder provide a sufficient thermal coupling between the sample holder and mixing chamber at low temperatures. Therefore, the sample holder is precooled down to about 20 K with H_2 as the exchange gas. It was checked experimentally that the thermal coupling occurs through nylon threads and not through NbTi wires.

The choice of the thermal link is a compromise between two conflicting requirements. In fact, the value of R_L must be rather large since C_T is very small and, as we noticed, a suitably large time constant is needed; small values of R_L would be necessary to avoid an excessively large temperature drop $\Delta T = R \cdot P$ between mixing chamber and sample holder to prevent parasitic pick up.

In the case of this example, a heat leak of $P = 1$ nW resulted in $\Delta T \approx 50$ mK. Heat pulses (with a duration of $\tau_H \approx 10$ ms at 0.1 K and 0.1 s at 1 K) were applied with a conventional pulse generator.

The energy input $\Delta Q = (V^2/R_H) \tau_H$ was determined by a measurement of V , R_H and τ_H . The power dissipation in the Si thermometer could be kept below 10^{-14} W.

The expression [3, 34]

$$T = T_0 e^{-\left[\frac{\ln(\ln(R/R_0))}{A_0} \right]} \quad (2.4)$$

was used to fit the data points, resistance R versus temperature T , with the constants T_0 , R_0 and A_0 determined by the fit [35].

From the curve $\Delta T(t) = T_i - T(t)$ (where T_i is the stationary initial temperature value before the heat pulse), the temperature difference ΔT can be obtained by extrapolating the $\Delta T(t)$ curve to zero time (see Fig. 2.2).

The heat capacity of the empty sample holder (addendum) was $C_{add} = aT + bT^3$ with $a = 5.6 \cdot 10^{-8}$ J K $^{-2}$ and $b = 9.9 \cdot 10^{-8}$ J K $^{-4}$. The T^3 contribution to C_{add} is explained quantitatively with the Debye heat capacity of the Si plate plus a small contribution arising from the Au wires, grease and contribution of one-third of heat capacity of the nylon threads. The linear term of C_{add} arises instead from the conductors (Si, Au), from insulators (grease and nylon) and the remaining contribution ($\approx 2 \cdot 10^{-8}$ J K $^{-2}$) probably stems from the degenerate n pads of the Si thermometer. A contribution of the same size has been previously observed in Si thermometers [36].

The resulting measurements carried out by this apparatus are shown in Fig. 2.4.

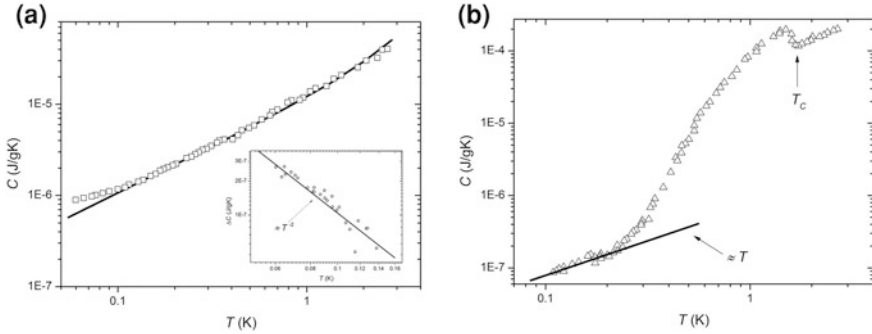
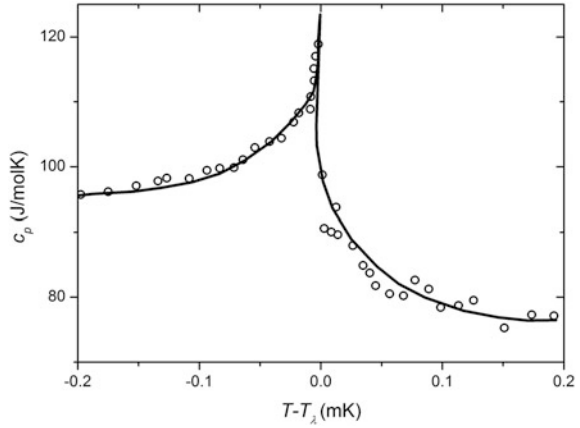


Fig. 2.4 **a** Specific heat C of Cu as a function of temperature T (log–log), of 40 mg Cu. The *solid line* indicates the Cu standard reference as determined between 0.4 and 3 K. The *inset* shows the observed additional contribution $\Delta C = C - \gamma T - \beta T^3$. **b** Specific heat C of amorphous $\text{Zr}_{65}\text{Cu}_{35}$ as a function of temperature T (log–log). The arrow marked T_c indicates the superconductive transition as determined resistively [33]

2.3.2 Example 2: Heat Pulse Calorimetry for the Measurement of the Specific Heat of Liquid ^4He Near its Superfluid Transition

One of the most interesting measurements using heat pulse calorimetry was carried out onboard the Space Shuttle (October 1992) [32]. The objective of the mission was to measure the specific heat at a constant pressure of liquid ^4He near its superfluid transition with the effect of gravity removed [37, 38]. In these experiments, C was measured with sub-nanokelvin resolution at temperatures within one nanokelvin of the transition temperature $T_\lambda = 2.177$ K. Such an extreme temperature resolution is only meaningful for the investigation of a phase transition of liquid helium because purity is high enough only in this substance, and thus the phase transition shows the required sharpness. In all other materials, the phase transitions are smeared by impurities and by imperfections of the structure. In addition, these measurements had to be carried out in reduced gravity in order to decrease the rounding of the transition caused by gravitationally induced pressure gradients and therefore spreading the transition temperature over the liquid sample of finite height. The high-resolution magnetic susceptibility thermometers developed for these experiments are described in [39]. In these experiments, the temperature stability was extremely important: in the experimental setup, four thermal control stages in series with the calorimeter were actively regulated in temperature: a stability of less than 0.1 nK/h was reached. Besides this thermal regulation, the experiment required a very careful magnetic shielding, in particular, of the electric leads, as well as extremely low electric noise levels. Figure 2.5 shows averaged data of the heat capacity close to the ^4He transition.

Fig. 2.5 Averaged data close to the transition. The continuous line shows the best-fit function [38]



2.4 Relaxation Calorimetry

A relaxation calorimeter (isoperibol) measures the total heat capacity (sample and addenda) by using a simple relation

$$C = \kappa \cdot \tau \quad (2.5)$$

where κ is the thermal conductance of the weak link between the platform and the thermal reservoir and τ is the constant of the temperature relaxation time of the platform.

Referring again to Fig. 1.22, a sample of heat capacity C_S and temperature T_S is fixed on a sample holder of heat capacity C_{SH} and temperature T_{SH} . Initially, for sake of simplicity, the sample and the sample holder are supposed to be isothermal. R_{SH} is the thermal resistance between the sample and the sample holder. The sample holder, whose temperature is measured by a thermometer T_{SH} , is connected to a heat bath at T_{Tb} by a link of thermal conductance R_{Tb} and negligible heat capacity. A constant power P_0 is applied to the sample holder until thermal equilibrium is achieved. At $t = t_1$, the power is switched off and the sample temperature T_S relaxes toward T_{Tb} . In the hypothesis that $R_{Tb} \gg R_{SH}$, the sample temperature follows

$$T_S(t) - T_{Tb} = P_0 R_{Tb} e^{(-t/(C_S + C_{SH})R_{Tb})} = \Delta T e^{(-t/\tau)}. \quad (2.6)$$

Changing T_{Tb} and repeating the measurement, a set of points for $C(T) = (C_S + C_{SH})(T)$ is obtained. The temperature difference ΔT must be kept as small as possible, usually a few percent of T_{Tb} , in order to ensure that τ can be considered as a constant. Practical values of τ range between about 1 and 1,000 s.

At very low temperatures, the thermal resistance R_{SH} between the sample and the holder can no longer be neglected because its temperature dependence usually becomes steeper than that of R_{Tb} . This introduces a second time constant τ_2 and the decay is described by

$$T_S(t) - T_{Tb} = A_1 e^{(-t/\tau_1)} + A_2 e^{(-t/\tau_2)} \quad (2.7)$$

where

$$A_1 + A_2 = \Delta T = P_0 \cdot R_{Tb}. \quad (2.8)$$

Equation (2.7) can be solved [40] to give

$$C_S + C_{SH} = K \left(\frac{A_1 \tau_1 + A_2 \tau_2}{A_1 + A_2} \right). \quad (2.9)$$

In realistic situations, τ_2 is much smaller than τ_1 and cannot be measured with enough accuracy to use Eq. (2.9). Reference [40] gives the useful approximation

$$C_S + C_{SH} \approx \left(A_1 \tau_1 / \Delta T \right) R_{Tb} \quad (2.10)$$

which is accurate in most cases within a few percent and avoids the need of calculating τ_2 . It is worth noting that the above-described “lumped τ_2 effect” is not the so-called “distributed τ_2 effect” due to low thermal conductivity of the sample itself. This latter case is discussed in [3, 34].

A variation of the relaxation method (see Sect. 2.5) was proposed by Riegel and Weber [41]. They describe a long (about 10 h) cycle to measure C over several degrees. In this method, they use an extremely weak thermal link to the heat sink and record the temperature of the sample while heating at constant power for one-half of the cycle, then allow the sample to relax while recording the temperature during the second half of the cycle with zero power input. The heat loss to the bath and surrounding can be eliminated from the calculation of C using this technique, provided the bath temperature can be held constant over the 10 h cycle. Note that this procedure is a particular case of the dual slope method of Sect. 2.5.

In [42, 43], the relaxation method is used with an amorphous silicon-nitride membrane, supported by a silicon frame, onto which thin-film heaters and thermometers (Pt for $T > 50$ K, amorphous NbSi or B doped Si for lower temperatures) are patterned. The heat capacity of this addendum is <1 nJ K⁻¹ at 2 K and only 6 μ J K⁻¹ at 300 K. This calorimeter was used to investigate microgram samples or thin films in steady fields up to 8T; according to the authors, it should also be usable in pulsed fields up to 60T. This is the result of the rather weak dependence of the properties of the calorimeter parts on magnetic field.

Finally, in [44], the heat capacity of holes in heavily doped Ge samples was measured using the relaxation method, an approximated “addendum free” configuration was obtained using a Ge thermometer with the same doping as the sample and extremely low capacity addendum components. We report the description of this experiment in some detail in Sect. 2.4.1.

The limitations of the thermal-relaxation method in properly measuring sharp features in the specific heat are illustrated, e.g., by the measurements of the

specific heat in the proximity of the first-order antiferromagnetic transition at $T = 14$ K in Sm_2IrIn_8 [45].

The relaxation method has been used for measurement of the specific heat of several materials as reported in [46, 47] (15–300 K, based on a closed cycle cryocooler) and also in [3, 34, 35, 38, 44, 48–59].

2.4.1 Example: Measurement of Specific Heat of Heavily Doped (NTD) Ge

The heat capacity of a NTD (Neutron Transmutation Doped, Ge 34B) Ge sample [60], 3 mm thick and with a diameter of about 3 cm (12.043 g), was measured in the 24–80 mK temperature range using the relaxation method [44].

In the realization of the experiment, authors approximated an “addendum free” configuration (see Table 1.7). The experimental setup is shown in Fig. 2.6.

The Ge wafer sample was glued with small spots of GE-varnish onto a Cu holder in good thermal contact with the mixing chamber of a dilution refrigerator. Three Kapton foils ($2 \times 2 \times 0.01$ mm³ each) electrically isolated the Ge wafer samples from the holder and realized the thermal conductance $G(T)$ between the samples and the heat sink.

For the two runs (described later), a calibrated NTD Ge #34B thermistor (same material of the sample, $3 \times 3 \times 1$ mm³) and a Si heater were used. Electrical connections were made by means of superconducting NbTi wires 25 μm in diameter. The connections between the gold wires of both thermistor and heater, and the NbTi leads were done by crimping the wires in a short Al tube (0.1 mg). At the ends of the NbTi wires, a four lead connection was adopted. An AVS47 AC resistance bridge was used for the thermometry, while a four-wire I – V source-meter (Keithley 236) supplied the current for the Si heater.

The addendum (represented by heater, glue spots, and Al tubes) gave a negligible contribution to the total heat capacity (see Table 2.2). The thermistor heat capacity was instead considered as part of the sample. The whole experiment was surrounded by a Cu shield at the mixing chamber temperature, measured by a calibrated RuO_2 thermometer.

Two measurements of heat capacity were carried out at different temperature range: (1) from 24 to 40 mK, (2) from 40 to 80 mK. For the two runs, the thermal conductance between the Ge wafers and the heat sink was measured by a standard integral method (see Ref. [2]).

The best fits of the values obtained in the two runs were

$$\begin{cases} G_1(T) = 1.22 \cdot 10^{-4} \cdot T^{2.52} [\text{WK}^{-1}] \\ G_2(T) = 3.05 \cdot 10^{-5} \cdot T^{2.45} [\text{WK}^{-1}] \end{cases} \quad (2.11)$$

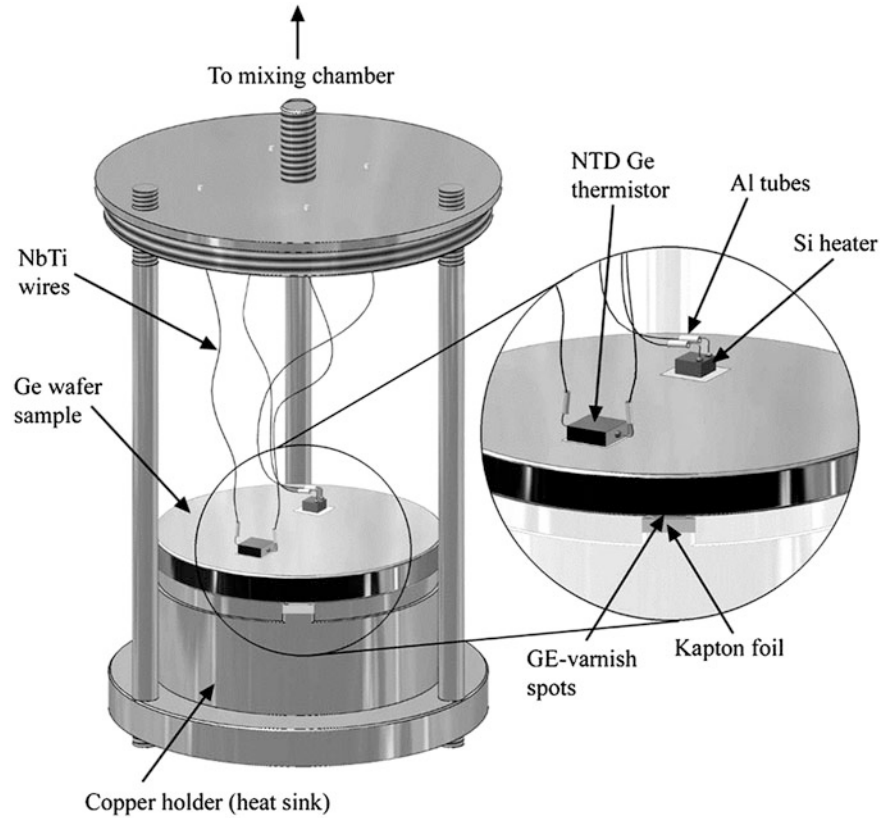


Fig. 2.6 Experimental setup of Ref. [44]

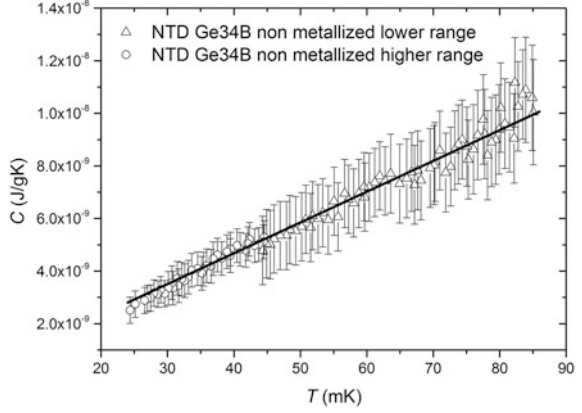
Table 2.2 Estimated heat capacity contributions. Specific heat data references are in [61]

Material	Volume (mm ³)	C (50 mK) (J K ⁻¹)	C (40 mK) (J K ⁻¹)	C (30 mK) (J K ⁻¹)
NTD Ge (electrons)	1950	10^{-7}	8×10^{-8}	6×10^{-8}
NTD Ge (phonons)	1950	6.8×10^{-10}	3.6×10^{-10}	1.5×10^{-10}
GE-varnish	0.52	1.8×10^{-10}	1.45×10^{-10}	1.1×10^{-10}
Al tubes	0.157	2.65×10^{-13}	1.36×10^{-13}	6×10^{-14}
NbTi wires	0.12	10^{-12}	5.4×10^{-13}	2.3×10^{-13}

The value of the heat capacity was calculated from equation $C = \tau \cdot G$, where the thermal time constant τ is obtained from the fit to the exponential relaxation of the wafer temperature.

Using the known thermal conductivity data of the wafer, the internal thermal relaxation time was estimated to be less than 1 ms, i.e., much shorter than C/G .

Fig. 2.7 Heat capacity per gram of the NTD Ge wafer. The *black line* represents the linear fitting



Such an estimate was confirmed by the fact that within the experimental errors, a single discharge time constant τ was always observed [61].

Since in the measured temperature range the Debye temperature of Ge is ~ 370 K, the phonon contribution to the heat capacity can be neglected [62]. Hence, the heat capacity of the samples is expected to be substantially influenced by only electron contribution, thus giving a linear dependence from T (see Sect. 1.2).

Let us consider data from the two measurements (see Fig. 2.7). Data can be well represented by a linear fit which crosses the origin within the experimental errors. The heat capacity per unit volume of the wafer sample is expressed by the following formula in the measured temperature range of 24–80 mK:

$$c(T) = (1.22 \pm 0.01) \cdot 10^{-7} [JK^{-1}g^{-1}]. \quad (2.12)$$

We can express specific heat in terms of volume:

$$c(T) = \gamma \cdot T = (7.52 \pm 0.08) \cdot 10^{-7} T [J K^{-1}cm^{-3}]. \quad (2.13)$$

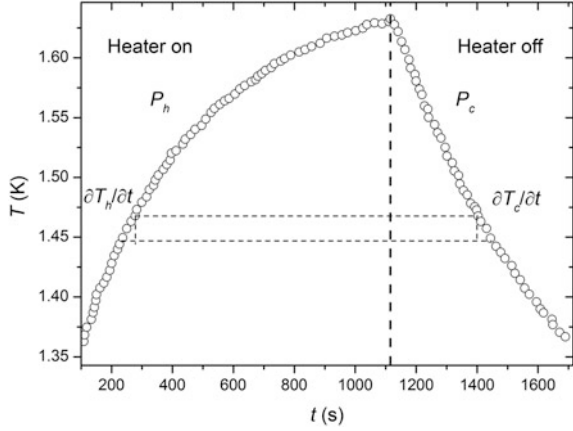
The value of γ is close to most of the Sommerfeld constant values reported in the literature for the NTD Ge of similar doping [63–66]. Note that the theoretical dependence of γ on the compensated dopant concentration is $p_c^{1/3}$ [67].

2.5 Dual Slope Method

In this method (isoperibol), C_p is evaluated by directly comparing the heating and cooling rates of the sample temperature without need of measuring the thermal conductance between sample and bath.

The heat capacity can be measured continuously through an extended temperature range, making use of both the heating and the cooling curves. This so-

Fig. 2.8 Example of the charge–discharge of heat power in the dual slope method



called Dual Slope (DS) method was proposed by Riegel and Weber [41], and Marcenat [68]. It consists of applying a heating power $P(t)$ to the sample holder (see Fig. 2.8) while continuously monitoring the sample temperature. For experimental setup in which the resistance between sample and holder is almost zero ($R_{SH} \approx 0$), the equations describing the heating and cooling curves, respectively, are

$$C(T) \frac{dT_h(T)}{dt} = P_h(T) - P_l(T) + P_p(T) \quad (2.14)$$

$$C(T) \frac{\partial T_c(T)}{\partial t} = -P_l(T) + P_p(T). \quad (2.15)$$

If we assume that in all the experiments the parasitic power ($P_p(T)$) and the power loss via heat link ($P_l(T)$) only depend on T and T_0 , it is possible to obtain $C(T)$ as

$$C(T) = \frac{P_h(T)}{\frac{\partial T_h(T)}{\partial t} - \frac{\partial T_c(T)}{\partial t}}. \quad (2.16)$$

Thus, the heat capacity of the sample at a certain temperature T can be obtained from the slope of the heating and cooling curves measured at T . It is worth noting that in (2.8), (2.9), and (2.10), the notation $C(T)$ indicates the total heat capacity that has to be split in two contributions: the first from the holder ($C_{SH}(T)$) and the second from the sample ($C_S(T)$).

In Fig. 2.8, an example of power charge and discharge is reported.

The method is very useful for making a quick scan through a large temperature range when the shape of the heat capacity curve is unknown, and considerably speeds up further measurements. As can be seen in (2.10), the dual slope method is self-correcting regarding parasitic heat leaks. Moreover, it is not necessary to explicitly know the thermal conduction of the heat link, although in most cases, the

measurement of $1/R_{Tb} = P_0/\Delta T$ is easily performed and this quantity can provide useful additional information for the data analysis. The frequencies with which the data points are taken will have to be adjusted to meet the requirement that when using this method, the derivatives with respect to the time of the sample temperature must be determined with great accuracy.

Also, in this method, poor thermal contact between the sample and sample holder can introduce a second time constant. In that case, it is still possible to retrieve $C(T)$ if an accurate determination of the second derivatives to the time of $T_h(t)$ and $T_c(t)$ can be made. The latter determination is often very difficult and one usually has to restrict the use of the DS method to those temperatures at which the influence of R_{SH} can be neglected.

Although the DS method is very elegant and easy to implement, the technique has usually been employed for small samples (typically less than 0.5 g) with good thermal conductivity and at temperatures lower than 20 K. The success of this method heavily depends on achieving an excellent thermal equilibrium between the sample, sample holder, and the thermometer, and for large samples with poor thermal conductivity (i.e., large τ_2), this method may also fail when we only consider the first-order approximation of the heat balance equations. Nevertheless, the DS method has been successfully used around 1 K, reducing to a minimum C_{SH} [49].

A slightly less sensitive method (variation of the dual slope) involving a fixed heat input followed by a temperature decay measurement is described in Ref. [47]. In this method, the sample is raised to an equilibrium temperature above the thermal bath and then allowed to relax to the bath temperature with no heat input. The method requires extensive calibration or the heat losses of the sample as a function of temperature between the reservoir and final sample temperature and relies on accurate, smooth temperature calibrations of thermometers because the time derivative of the temperature during the decay process is necessary to extract the specific heat. A data analysis method designed to eliminate the calculation of the time derivative of the temperature during the decay was also described in Ref. [47]. The technique requires a determination of many equilibrium heat losses during the heating portion of the relaxation cycle to obtain good temperature resolution of the specific heat changes.

A modification of the DS technique which is a hybrid between the AC method and the DS method and reduces the duration of the measuring cycle has been proposed in Ref. [69]. The method which was devised to measure specific heats of small samples has good sensitivity and can give many points on the heat capacity versus temperature curve during one cycle of about a 2 h duration covering a temperature range of several K.

As stated, the DS method is time consuming both in performing measurements and for data analysis. For these reasons, it has been used less than other methods, despite the inherent advantages hereafter described. Some examples are reported in [41, 49, 69–71].

2.6 AC Calorimetry

AC calorimetry (isoperibol, also known as modulation calorimetry, TMC) consists of generating a periodic oscillation of power $P(t)$ with the frequency 2ω that heats the sample of heat capacity C_S and in recording the resulting temperature oscillations $T_S(t)$ as a function of time. The measured temperature oscillates with the same frequency and amplitude $\Delta T_S(t)$ around a mean temperature T_M . A phase shift φ develops between $P(t)$ and $T_S(t)$ due to the finite thermal resistance R_{tb} between the sample and thermal bath, T_{Tb} . The scheme of such a calorimeter is the same as in Fig. 1.22 with some differences and is shown in Fig. 2.9.

The basic relations for a modulation calorimeter result from the following common equation that describes, in its simplest form, any calorimetric system

$$P(t) = C_S \left(\frac{dT_S}{dt} \right) + K_{Tb}(T_S - T_{Tb}) \quad (2.17)$$

where $K_{Tb} = 1/R_{Tb}$.

If one drives the heater with a current $I = I_0 \cos(\omega t)$, Joule heating occurs at a frequency 2ω at the heater. Equation (2.11) becomes

$$P(t) = P_{AC} e^{i2\omega t} = 2i\omega C_S \Delta T^*(t) e^{2i\omega t} + K_{Tb} \Delta T^*(t) e^{2i\omega t} \quad (2.18)$$

where ΔT^* denotes the complex amplitude of the temperature oscillation.

The solution $\Delta T(t)$ can be written as

$$\Delta T_{AC}(t) = \Delta T^* e^{i\omega t} = |^*| e^{i\varphi} e^{i\omega t}. \quad (2.19)$$

Introducing the complex heat capacity as $C_S^* = C' - iC''$, the temperature oscillation and the phase shift (between power and temperature) are given by the following equations:

$$C' = -\frac{P_{AC}}{2\omega |\Delta T^*|} \sin \varphi \quad (2.20)$$

$$C'' = -\frac{P_{AC}}{2\omega |\Delta T^*|} \cos \varphi - \frac{K_B}{2\omega} \quad (2.21)$$

$$|\Delta T^*| \equiv \frac{P_{AC}}{\sqrt{(2\omega C_S)^2 + K_{Tb}^2}} \quad (2.22)$$

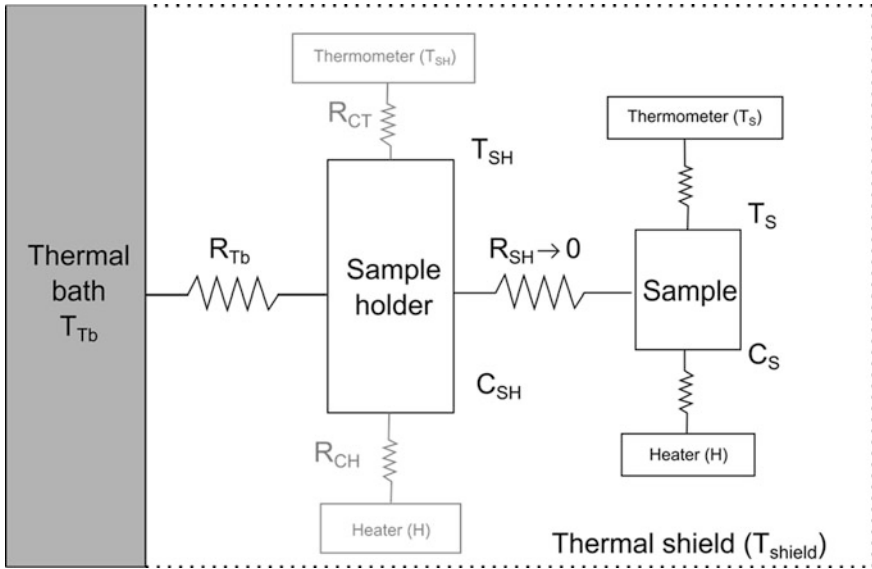


Fig. 2.9 Scheme of a calorimetric measuring cell. T_{Tb} temperature of the bath, T_{shield} temperature of heat shield, T_S temperature of the sample, R_{Tb} thermal resistance towards thermal bath, and C_S sample heat capacity. Note that R_H is neglected

with

$$K_{Tb} = [P_{AC}/|\Delta T^*|] \cos \varphi \quad (2.23)$$

$$\varphi = \arctan\{2\omega C_S/K_{Tb}\}. \quad (2.24)$$

If the thermometer is connected to the sample without thermal resistance and the sample is thought of as isothermal, amplitude of the thermal oscillations is the same through the sample and $C'' = 0$.

Let us note that the modulation method requires either a heat loss by conduction to the thermal bath through R_{Tb} or by radiative cooling toward the shield. As a consequence, AC calorimetry can never operate under adiabatic conditions and there always exists a heat flow from the sample to the thermal bath through a radiation resistance R_{Tb} . If $R_{Tb} \gg \omega C_S$, (2.16) yields $\Delta T_{AC} \approx P_{AC}/\omega C_S$ and the phase approaches the value $\varphi = -(\pi/2)$. These are the usual working conditions of a traditional AC calorimeter and in this case, the system works under quasiadiabatic conditions [72]. For all other cases, heat losses and phase shifts between input power and sample temperature must be taken into account using the full formula (2.16).

Finally, according to all of the above-mentioned equations, the oscillations are superimposed by a temperature increase $\Delta T_{DC} = P_{AC} R_{Tb}/2$. We note that in contrast to other calorimetric methods, in the AC calorimetry, the sample can be located in vacuum or in exchange gas. Also, modulation is not restricted to sinusoidal

oscillations, but can have any other waveform, e.g., rectangular or triangular wave forms have been used [18, 19, 73]. Modulation can also be induced indirectly to the sample by giving a modulated power to the heat shield [20].

A modification of the TMC technique (the 3ω -method) is based on the original work by Corbino [74]. Later, Rosenthal [75] and Filippov [76] used the bridge technique to measure third harmonic signals. In the original work in 1910–1911, Corbino [74] used the resistance of electrically conducting samples to determine the temperature oscillations with a method known as the third-harmonic (3ω) method. In this kind of experiment, the same metal resistor element is used as both a heater and thermometer. The heater, with resistance R , is driven by a current at frequency ω which results in a power of 2ω frequency that causes diffusive thermal waves which perturb the sensor resistance. The combined effect of driving current and resistance oscillations gives a voltage across the resistor in a form containing a first term which is the normal AC voltage at the drive frequency, while the second and third terms, which derive the current and resistance oscillations from mixing, are dependent on the ΔT , (the temperature oscillation amplitude, which, in turn, is related to the sample heat capacity) [77].

Although the 3ω signal is relatively small (see, e.g., [72]) compared to the two terms (oscillating with ω and 2ω), it can be well separated by the lock-in technique. For more experimental details, refer to [20, 78–82]. Measurements using AC calorimetry are reported, e.g., [83–88].

2.7 Differential Scanning Calorimetry

A precious tool for investigating the thermodynamics of chemical reactions and phase transitions is the differential thermal-analysis (DTA) technique, which is widely used in chemical and material sciences. In a typical experiment, the specimen and a reference material of similar heat capacity are heated simultaneously. If the two samples are sufficiently thermally insulated from each other, changes in the temperature difference between the sample and the reference material reflect heat capacity variations or indicate the occurrence of chemical reactions. Typical heating rates are of the order of several degrees per minute. Under such conditions, however, the samples are not always in thermal equilibrium. The resulting problems related to the geometry of the samples and the sample holders make a calculation of absolute heat-capacity data rather complicated, and it is therefore rarely done in practice [3].

The use of high-precision (magnetic field independent) electronic components makes it possible to achieve a relative accuracy $\Delta C/C < 0.02\%$ on samples of milligram weight. This accuracy is at least of the same order of magnitude as that reached with the frequently used continuous-heating technique where significantly larger sample masses are usually required. Moreover, the method is time saving and very simple to apply since neither calibration nor a very precise temperature

regulation is necessary in principle. Heat-capacity measurements can be done upon heating or cooling the samples.

We shall describe the principle of the measurement [89] referring to the configuration shown in Fig. 2.10. The sample (with heat capacity C_S at a temperature T_S) and a reference sample (at a temperature T_R , with known heat capacity C_R) are thermally connected to a sample holder (temperature T_{SH}) directly anchored to a heat reservoir (usually $T_{Tb} = T_{SH}$, and hence the heater H acts on the sample holder and on thermal bath) via the heat links R_{SH} and R_{RH} , respectively. We might also include a thermal connection R_{SR} between the sample and the reference object, but it is possible to thermally isolate the two specimens from each other in a real experiment, i.e., $R_{SR} \gg R_{SH}, R_{RH}$. Results of a calculation taking the effect or a nonzero thermal conductance between the sample and the reference into account are discussed in an Appendix to [89].

If the temperature of the sample holder T_{SH} varies with time, it is possible to describe the system by

$$C_S T = k_S (T_{SH} - T_S) \quad (2.25)$$

$$C_R T_R = k_{RH} (T_{SH} - T_R) \quad (2.26)$$

where $k_{SH} = 1/R_{SH}$ and $k_{RH} = 1/R_{RH}$. It is instructive to first consider steady-state solutions of (2.25) and (2.26) when C_S and C_R are assumed to be temperature independent, and $T_{SH}(t)$ is a linear function of time. In order to avoid the thermal equilibrium problems, we choose the characteristic time constants of the system. $T_j = C_j/k_j$ (with $j = S$ or R) to be larger than the internal equilibrium times of the samples, τ_{int} which are typically less than 1 s at $T = 100$ K. In a straightforward manner, we obtain $T_S = T_R = T_{SH}$ and $T_{SH} - T_j = C_j T_{SH}/k_j$. Assuming identical heat links ($k_s = k_r$), we find that the quantity

$$\Delta C_0 = C_R [(T_S - T_R)/(T_R - T_{SH})] \quad (2.27)$$

asymptotically approaches the heat-capacity difference $\Delta C = C_S - C_R$ at times $t \gg \tau_j$ after switching on the linear temperature ramp $T_{SH}(t)$. In a more realistic contest, the heat capacities C_S and C_R are temperature dependent, and $T_{SH}(t)$ may deviate from linearity. It may then be argued that ΔC_0 still approaches ΔC for $t \gg \tau_j$ as long as heat-capacity changes and variations of T_{SH} in time are sufficiently slow, i.e., occur on a time scale much larger than τ_j . The DTA technique has been used, e.g., in [90, 91].

A remarkable advantage of DSC is that it is easy to measure the temperatures T_S , T_R and T_{SH} in an experiment; thus, if $k_{SH} = k_{RH}$, then ΔC_0 calculated according to (2.27) represents an excellent approximation for the heat-capacity difference, and can be determined without knowledge of the absolute values of k_{SH} and k_{RH} .

Note, however, that a sharp feature in the quantity C_S and thus in ΔC will be smeared out due to the finite thermal relaxation of the system. This occurs on the time scale $\tau_s = C_S/k_s$. Within this time, the sample will be heated approximately

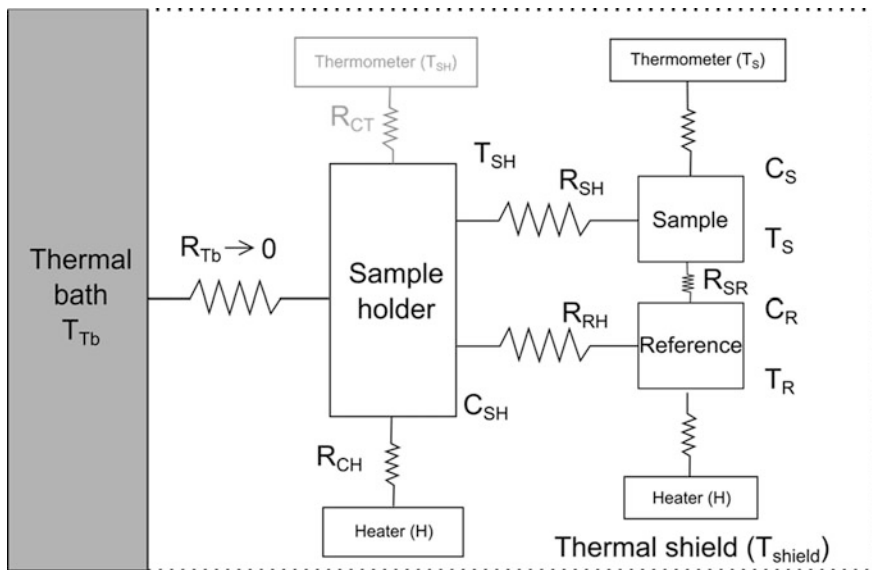


Fig. 2.10 Schematic of DTA configuration. The sample (heat capacity C_S , temperature T_S) and the reference sample (heat capacity C_R , temperature T_R) are thermally connected to the sample holder (temperature T_{Tb}) through the heat links R_{SH} , R_{RH} . The effect of an unwanted link R_{SR} is discussed in Ref. [89]. R_{Tb} is usually neglected

by the quantity $\tau_s dT_S/dt = \tau_b dT_{Tb}/dt = T_{Tb} - T_s$, which is therefore a measure for the resulting broadening effect on $\Delta C_0(T)$ on the temperature axis. According to (2.27), $\Delta C/C_R$ can be determined within this instrumental uncertainty simply by simultaneously monitoring the three temperatures T_R , T_S and T_{SH} , without calculating any derivative in time or in temperature. The aforementioned limit $(T_{Tb} - T_s)$ in the instrumental temperature resolution for $\Delta C_0(T)$ can be reduced by slowing down the variation $T_{SH}(t)$ of the heat reservoir since $T_{SH} - T_s = (dT_{SH}/dt)C_S/k_{SH}$.

Another remarkable achievement reported in [89] is said to be the substantial improvement of the conventional differential thermal-analysis (DTA) method by means of using high-precision electronics and careful temperature control. This method was used to measure the heat capacity of milligram samples at low temperatures and in magnetic fields up to 7 T with a relative accuracy of about 10^{-4} .

References about DSC are [92–94].

2.8 Other Methods

Besides the methods for measuring the heat capacity described in the previous sections, other methods have been proposed and used. Among them, it is worth citing:

- (a) Nonadiabatic measurements of the heat capacity involving sample-inherent thermometry proposed in [95]. The method is realized with a superconducting quantum interference magnetometry device and applied to FeBr_2 single crystals by using the magnetization for both thermometry and relaxation calorimetry.
- (b) Modulated-bath calorimetry [96] is a variation of the AC calorimetric technique for measuring the absolute heat capacity of extremely small samples. The method uses a thermocouple as the weak link to the bath and modulates the temperature of the bath in time. This eliminates the need for a separate thermometer and heater on the sample while retaining the ability to make absolute measurements with minimal addenda.

2.9 Industrial Calorimeters

We also wish to mention the automated heat-capacity measurement system (for samples weighing 10–500 mg) manufactured by Quantum Design [97] which employs a thermal-relaxation calorimeter and operates in the temperature range of 1.8–395 K. Examples of measurements carried out by means of this instrument are reported in [98, 99]. The system also allows one to perform very sensitive electric and magnetic measurements (e.g., AC susceptibility and DC magnetization). It employs the thermal relaxation method in the temperature range 1.8–395 K (optional 0.35–350 K with a continuously operating closed-cycle ^3He system). As an option, it can be equipped for measurements in magnetic field up to 16 T longitudinal or 7 T transverse. Its calorimeter platform consists of a thin alumina square of $3 \times 3 \text{ mm}^2$, backed by a thin-film heater and a bare Cernox (cryogenic thermometers fabricated from sputtered zirconium oxynitride thin films, commercially available from Lake Shore Cryotronics, Inc. under the trademark CernoxTM). A heat pulse is applied and the platform temperature is recorded. With known values for the conductance of the thermal link to the bath, of the heat capacity of the addendum, and of the applied heat, the heat capacity of the sample and the internal time constant of the calorimeter are determined analytically from the $T(t)$ data by numerically integrating the relevant differential equations. The curve fitting is improved by carrying out a number of decay sweeps at each temperature and averaging the results. Two Cernox thermometers are used over the full temperature range and their calibration is based on the ITS-90 temperature scale [100]. The resolution of the system is 10 nJK^{-1} at 2 K. According to an examination of the system, the accuracy is 1 % at 10–300 K, which decreases to about $\sim 5 \%$ at $T < 5 \text{ K}$. The system is quite adequate to describe broad second-order phase transitions; however, sharp first-order transitions cannot be investigated properly, mainly because the applied software cannot describe nonexponential decay curves. This drawback can be removed by using an alternate analytic approach [97]. The system has recently been equipped with a simple, fully-

automated dilution refrigerator for heat-capacity measurements from 55 mK to 4 K and in fields up to 9 T.

Recommendations for the use of quantum devices are reported in Ref. [101].

2.10 Small Sample Calorimetry

With reference to (2.2), cryogenic calorimeters are not only used to measure heat capacities of liquids and solids, but also in a variety of other applications like the detection of weakly interacting massive particles, of x-rays and γ -rays, and in astrophysics, or as bolometers for detection of phonons, particles or electromagnetic waves, and particularly for detection of infrared radiation. These applications have emerged from the very high sensitivity of recent microcalorimeters capable of measuring C in the range of nJ/K (corresponding to the heat capacity of a monolayer of ^4He , see, e.g., [101]) or even less. For a review on these devices and their applications, see, e.g., [2, 102].

The study of novel materials, many of which can be obtained in only small amounts, has benefited from small-sample calorimetric measurements. These types of measurements are usually made using the AC method developed by Handler and coworkers in 1967 [82] and Sullivan and Seidel in 1968 [87], or by a thermal relaxation method developed by Bachmann et al. in 1972, [3] as amply discussed in the preceding sections.

Independently of the adopted technique, the absolute accuracy of any measurement of heat capacity is limited by the fraction of the total C which is not due to the sample, i.e., the addenda. The last 20 years has seen a continuous decrease in the mass of the measurable sample, mostly because of decreases in the addenda contribution (particularly of thermometers).

The silicon bolometer described in Ref. [103] enabled one to measure a 1 mg sample in 1972 [36]; it consisted of approximately 25 mg of silicon divided into two sections. Both sections had phosphorous diffused into the surface and then etched to give a concentration versus depth profile such that one section had a resistance of several kilo-ohms at 4.2 K and the other a resistance of several tens of kilo-ohms at 4.2 K. Thus, the combination of two thermometers enabled a wider temperature range; the thermometer which was not in use at a given temperature was used as a heater. The next improvement in thermometer design was the use of a small chip of doped germanium attached to a thin sapphire disk which had sufficient area and strength to serve as a platform.

In the thermal relaxation method, [42, 43, 97, 104] the sensitivity is determined by the quality of the thermometer and by the (as small as possible) heat capacity of the addenda. This method can have rather high absolute accuracy; however, its relative accuracy is limited. On the contrary, the AC method can detect very small changes in the heat capacity [104–108]. As we saw in Sect. 2.6, the heating power waveform is usually sinusoidal and the resulting temperature oscillation at frequency ω is determined. It is

$$\Delta T = \frac{P}{\omega C \sqrt{l + \frac{1}{\omega^2 \tau_1^2} + \frac{1}{\omega^2 \tau_2^2}}} \quad (2.28)$$

where τ_2 is the relaxation time within the calorimeter assembly and τ_1 is the relaxation time of the calorimeter to the bath. In the usual limit $\omega \tau_1 \gg 1 \gg \omega \tau_2$, the heat capacity can be obtained as $C = P/\Delta T$. To check whether this limit has been achieved, the temperature response has to be measured at various frequencies (typically between 10 and 200 Hz) to determine below which frequency heat leaks through the thermal link to the bath (within the measuring period) and above which frequency the calorimeter can no follow the heat modulation. In other words, the pass-band of the calorimeter is measured.

A relaxation calorimeter for use in a top-loading ^3He - ^4He dilution refrigerator in high magnetic field has been described in Ref. [34]. It has been used for milligram samples from 34 mK to 3 K and in magnetic fields up to 18 T. In order to keep thermal time constants in the magnetic field reasonably short, most of the addenda, like the thermal reservoir, were made from Ag, which has a very low nuclear heat capacity.

Very sensitive microcalorimeters are described in [107–109]. The AC calorimeter of Ref. [86], for the Kelvin temperature range consists of a 2–10- μm -thick monocrystalline silicon membrane substrate produced by etching, taking advantage of the high thermal conductivity and low heat capacity at low temperatures of this material. A 150 nm CoNi heater (with temperature independent resistivity between 1 and 20 K) and a 150 nm NbN thermometer are deposited onto the substrate. The addenda of this calorimeter varied between less than 0.1 nJ/K at $T < 1$ K and some nJ/K at 4 K. The device was used to measure heat capacities of systems of deposited thin films or multilayers of microgram single crystals and eventually of mesoscopic superconducting loops. The achieved resolution of $\Delta C/C < 5 \times 10^{-5}$ allowed measurements of variations of C as small fJ/K [108].

A further improvement in the thermometer design was the silicon on sapphire (SOS) thermometer technique [110] in which phosphorous was ion-implanted into a 0.6 micron-thick Si layer on a 0.005-in.-thick sapphire substrate. Ion implantation allowed the concentration versus depth profile to be as desired, eliminating the inexact etching step. A third section had been added to the original bolometer design to serve as a heater. The SOS design is able to measure sample as light as 0.1 mg, to be compared to the 1 mg limit typical of the old silicon bolometer design.

Another innovation in sample platform thermometers that was quite similar to the SOS design is the use of a flash-evaporated thin Au–Ge layer (with low heat capacity) as a thermometer which adheres to the platform without the need for glue required in the Ge chip design. The aforementioned designs use wires which, even if the diameter is as small as 25 micron, make a significant addendum contribution [3]; all use a relatively massive sample platform, at least 10 mg, which, even if it is sapphire or diamond (with large Debye temperature, see Table 1.1), contributes a relatively large addendum.

For the development of small sample calorimetry, see, e.g., Ref. [15, 106, 111], where a combination of AC and heat-pulse calorimetry is used to measure the specific heat of the ceramic superconductor $\text{YBa}_2\text{Cu}_3\text{O}_{7-\delta}$ near the transition temperature $T_c = 90$ K.

As seen in Sect. 2.2, small sample calorimetry has now attained the nanogram range [112, 113].

References

1. Ventura, G., Lanzi, L., Peroni, I., Peruzzi, A., Ponti, G.: Low temperature thermal characteristics of thin-film Ni–Cr surface mount resistors. *Cryogenics* **38**(4), 453–454 (1998)
2. Ventura, G., Risegari, L.: *The art of cryogenics: low-temperature experimental techniques*. Elsevier, Amsterdam (2007)
3. Bachmann, R., DiSalvaio, F.J., Geballe, T.H., Greene, R.L., Howard, R.E., King, C.N., Kirsch, H.C., Lee, K.N., Schwall, R.E., Thomas, H.U., Zubeck, R.B.: Heat capacity measurements on small samples at low temperatures. *Rev. Sci. Instr.* **51**, 205 (1972)
4. Martin, D.L.: Use of pure copper as a standard substance for low temperature calorimetry. *Rev. Sci. Instrum.* **38**(12), 1738–1740 (1967)
5. Martin, D.L.: Specific heats below 3 K of pure copper, silver, and gold, and of extremely dilute gold-transition-metal alloys. *Phys. Rev.* **170**(3), 650–655 (1968)
6. Martin, D.L.: Tray type calorimeter for the 15–300 K temperature range: copper as a specific heat standard in this range. *Rev. Sci. Instrum.* **58**(4), 639–646 (1987)
7. Cetas, T.C., Tilford, C.R., Swenson, C.A.: Specific heats of Cu, GaAs, GaSb, InAs, and InSb from 1 to 30 K. *Phys. Rev.* **174**(3), 835–844 (1968)
8. Ahlers, G.: Heat capacity of copper. *Rev. Sci. Instrum.* **37**(4), 477–480 (1966)
9. Holste, J.C., Cetas, T.C., Swenson, C.A.: Effects of temperature scale differences on the analysis of heat capacity data: the specific heat of copper from 1 to 30 K. *Rev. Sci. Instrum.* **43**(4), 670–676 (1972)
10. Black, J., Robinson, J., Chemist, P., Britain, G.: *Lectures on the Elements of Chemistry, Delivered in the University of Edinburgh*. Mundell and Son for Longman and Rees, London, and William Creech, Edinburgh (1803)
11. Hansen, L.D.: Toward a standard nomenclature for calorimetry. *Thermochim. Acta* **371**(1), 19–22 (2001)
12. Zielenkiewicz, W.: Towards classification of calorimeters. *J. Therm. Anal. Calorim.* **91**(2), 663–671 (2008)
13. Kubaschewski, O., Alcock, C., Spencer, P.: *Materials Thermochemistry*, vol. 6. Pergamon Press, Oxford (1993)
14. Nernst, W.: The energy content of solids. *Ann Physik* **36**, 395–439 (1911)
15. Schnelle, W., Gmelin, E.: Critical review of small sample calorimetry: improvement by auto-adaptive thermal shield control. *Thermochim. Acta* **391**(1), 41–49 (2002)
16. Cardwell, D.A., Ginley, D.S.: *Handbook of superconducting materials*, vol. 1. CRC Press, Boca Raton (2003)
17. Kishi, A., Kato, R., Azumi, T., Okamoto, H., Maesono, A., Ishikawa, M., Hatta, I., Ikushima, A.: Measurement of specific heat anomaly and characterization of high TC ceramic superconductors by AC calorimetry. *Thermochim. Acta* **133**, 39–42 (1988)
18. Jin, X.C., Hor, P.H., Wu, M.K., Chu, C.W.: Modified high-pressure ac calorimetric technique. *Rev. Sci. Instrum.* **55**(6), 993–995 (1984)
19. Machado, F.L.A., Clark, W.G.: Ripple method: an application of the square-wave excitation method for heat-capacity measurements. *Rev. Sci. Instrum.* **59**(7), 1176–1181 (1988)

20. Kraftmakher, Y.A., Cherepanov, V.Y.: Compensation of heat losses in modulation measurements of specific heat. *Teplofiz. Vys. Temp.* **16**, 647–649 (1978)
21. Euken, A.: The determination of specific heats at low temperatures. *Physik. Z.* **10**, 586–589 (1909)
22. Nernst, W.: Sitzungsbericht der K. Preuss. Akad. Wiss **12**, 261 (1910)
23. Bagatskii, M.I., Minchina, I.Y., Manzhelii, V.G.: Specific heat of solid para-hydrogen. *Soviet J. Low Temp. Phys.* **10**, 542 (1984)
24. Ward, L.G., Saleh, A.M., Haase, D.G.: Specific heat of solid nitrogen-argon mixtures: 50 to 100 mol% N₂. *Phys. Rev. B* **27**(3), 1832–1838 (1983)
25. Alkhafaji, M.T., Migone, A.D.: Heat-capacity study of butane on graphite. *Phys. Rev. B* **53**(16), 11152–11158 (1996)
26. Sellers, G.J., Anderson, A.C.: Calorimetry below 1 K: the specific heat of copper. *Rev. Sci. Instrum.* **45**(10), 1256–1259 (1974)
27. Filler, R.L., Lindenfeld, P., Deutscher, G.: Specific heat and thermal conductivity measurements on thin films with a pulse method. *Rev. Sci. Instrum.* **46**(4), 439–442 (1975)
28. Harrison, J.P.: Cryostat for the measurement of thermal conductivity and specific heat between 0.05 and 2 K. *Rev. Sci. Instrum.* **39**(2), 145–152 (1968)
29. Morin, F.J., Maita, J.P.: Specific heats of transition metal superconductors. *Phys. Rev.* **129**(3), 1115–1120 (1963)
30. Al-Shibani, K.M., Sacli, O.A.: Low temperature specific heats of AgSb alloys. *Phys. Status Solidi B* **163**(1), 99–105 (1991). doi:[10.1002/pssb.2221630108](https://doi.org/10.1002/pssb.2221630108)
31. Osborne, D.W., Flotow, H.E., Schreiner, F.: Calibration and use of germanium resistance thermometers for precise heat capacity measurements from 1 to 25 K. high purity copper for interlaboratory heat capacity comparisons. *Rev. Sci. Instrum.* **38**(2), 159–168 (1967)
32. Hiroo, O., Toshiaki, E., Nobuhiko, W.: Heat capacity anomaly of Ag ultrafine particles at low temperatures. *J. Phys. Soc. Jpn.* **59**, 1695 (1990)
33. Albert, K., Löhneysen, H., Sander, W., Schink, H.: A calorimeter for small samples in the temperature range from 0.06 K to 3 K. *Cryogenics* **22**(8), 417–420 (1982)
34. Tsujii, H., Andracka, B., Muttalib, K., Takano, Y.: Distributed τ_2 effect in relaxation calorimetry. *Phys. B* **329**, 1552–1553 (2003)
35. Gutmiedl, P., Probst, C., Andres, K.: Low temperature calorimetry using an optical heating method. *Cryogenics* **31**(1), 54–57 (1991)
36. Greene, R.L., King, C.N., Zubeck, R.B., Hauser, J.J.: Specific heat of granular aluminium films. *Phys. Rev. B* **6**(9), 3297–3305 (1972)
37. Lipa, J., Swanson, D., Nissen, J., Chui, T.: Lambda point experiment in microgravity. *Cryogenics* **34**(5), 341–347 (1994)
38. Lipa, J., Nissen, J., Stricker, D., Swanson, D., Chui, T.: Specific heat of liquid helium in zero gravity very near the lambda point. *Phys. Rev. B* **68**(17), 174518 (2003)
39. Chui, T., Day, P., Hahn, I., Nash, A., Swanson, D., Nissen, J., Williamson, P., Lipa, J.: High resolution thermometers for ground and space applications. *Cryogenics* **34**, 417–420 (1994)
40. Shepherd, J.P.: Analysis of the lumped τ_2 effect in relaxation calorimetry. *Rev. Sci. Instrum.* **56**(2), 273–277 (1985)
41. Riegel, S., Weber, G.: A dual-slope method for specific heat measurements. *J. Phys. E: Sci. Instrum.* **19**(10), 790 (1986)
42. Zink, B.L., Revaz, B., Sappey, R., Hellman, F.: Thin film microcalorimeter for heat capacity measurements in high magnetic fields. *Rev. Sci. Instrum.* **73**(4), 1841–1844 (2002)
43. Denlinger, D.W., Abarra, E.N., Allen, K., Rooney, P.W., Messer, M.T., Watson, S.K., Hellman, F.: Thin film microcalorimeter for heat capacity measurements from 1.5 to 800 K. *Rev. Sci. Instrum.* **65**(4), 946–959 (1994)
44. Olivieri, E., Barucci, M., Beeman, J., Risegari, L., Ventura, G.: Excess heat capacity in NTD ge thermistors. *J. Low Temp. Phys.* **143**(3–4), 153–162 (2006)
45. Pagliuso, P.G., Thompson, J.D., Hundley, M.F., Sarrao, J.L., Fisk, Z.: Crystal structure and low-temperature magnetic properties of R_mMIn_{3 m + 2} compounds (M = Rh or Ir; m = 1,2; R = Sm or Gd). *Phys. Rev. B* **63**(5), 054426 (2001)

46. Catarino, I., Bonfait, G.: A simple calorimeter for fast adiabatic heat capacity measurements from 15 to 300 K based on closed cycle cryocooler. *Cryogenics* **40**(7), 425–430 (2000)
47. Forgan, E.M., Nedjat, S.: Heat capacity cryostat and novel methods of analysis for small specimens in the 1.5–10 K range. *Rev. Sci. Instrum.* **51**(4), 411–417 (1980)
48. Barucci, M., Di Renzone, S., Olivieri, E., Risegari, L., Ventura, G.: Very-low temperature specific heat of Torlon. *Cryogenics* **46**(11), 767–770 (2006)
49. Willekers, R., Meijer, H., Mathu, F., Postma, H.: Calorimetry by means of the relaxation and dual-slope methods below 1 K: application to some high T_c superconductors. *Cryogenics* **31**(3), 168–173 (1991)
50. Drulis, M.: Low temperature heat capacity measurements of U_6FeH_{15} hydride. *J. Alloys Compd.* **219**(1), 41–44 (1995)
51. Barucci, M., Brofferio, C., Giuliani, A., Gottardi, E., Peroni, I., Ventura, G.: Measurement of low temperature specific heat of crystalline TeO_2 for the optimization of bolometric detectors. *J. Low Temp. Phys.* **123**(5–6), 303–314 (2001). doi:[10.1023/a:1017555615150](https://doi.org/10.1023/a:1017555615150)
52. Kim, J.S., Stewart, G.R., Bauer, E.D., Ronning, F.: Unusual temperature dependence in the low-temperature specific heat of $U_3Ni_3Al_{19}$. *Phys. Rev. B* **78**(15), 153108 (2008)
53. Cinti, F., Affronte, M., Lascialfari, A., Barucci, M., Olivieri, E., Pasca, E., Rettori, A., Risegari, L., Ventura, G., Pini, M.G., Cuccoli, A., Roscilde, T., Caneschi, A., Gatteschi, D., Rovai, D.: Chiral and helical phase transitions in quasi-1d molecular magnets. *Polyhedron* **24**(16–17), 2568–2572 (2005)
54. Nakajima, Y., Li, G., Tamegai, T.: Specific heat study of ternary iron-silicide superconductor $Lu_2Fe_3Si_5$: evidence for two-gap superconductivity. *Physica C* **468**(15), 1138–1140 (2008)
55. Kasahara, S., Fujii, H., Mochiku, T., Takeya, H., Hirata, K.: Specific heat of novel ternary superconductors $La_3Ni_4X_4$ ($X = Si$ and Ge). *Physica C* **468**(15), 1231–1233 (2008)
56. Kasahara, S., Fujii, H., Mochiku, T., Takeya, H., Hirata, K.: Low temperature specific heat of ternary germanide superconductor $La_3Pd_4Ge_4$. *Phys. B* **403**(5), 1119–1121 (2008)
57. Kasahara, S., Fujii, H., Takeya, H., Mochiku, T., Thakur, A., Hirata, K.: Low temperature specific heat of superconducting ternary intermetallics $La_3Pd_4Ge_4$, $La_3Ni_4Si_4$, and $La_3Ni_4Ge_4$ with $U_3Ni_4Si_4$ -type structure. *J. Phys.: Condens. Matter* **20**(38), 385204 (2008)
58. Fanelli, V., Christianson, A.D., Jaime, M., Thompson, J., Suzuki, H., Lawrence, J.: Magnetic order in the induced magnetic moment system Pr_3In . *Phys. B* **403**(5), 1368–1370 (2008)
59. Suzuki, H., Inaba, A., Meingast, C.: Accurate heat capacity data at phase transitions from relaxation calorimetry. *Cryogenics* **50**(10), 693–699 (2010)
60. Haller, E.: Advanced far-infrared detectors. *Infrared Phys. Technol.* **35**(2), 127–146 (1994)
61. Lounasmaa, O.V. (ed.): *Experimental principles and methods below 1 K*. Academic Press, London (1974)
62. Keesom, P., Seidel, G.: Specific heat of germanium and silicon at low temperatures. *Phys. Rev.* **113**(1), 33 (1959)
63. Wang, N., Wellstood, F.C., Sadoulet, B., Haller, E.E., Beeman, J.: Electrical and thermal properties of neutron-transmutation-doped Ge at 20 mK. *Phys. Rev. B* **41**(6), 3761–3768 (1990)
64. Aubourg, É., Cummings, A., Shutt, T., Stockwell, W., Barnes Jr, P., Silva, A., Emes, J., Haller, E., Lange, A., Ross, R., Sadoulet, B., Smith, G., Wang, N., White, S., Young, B., Yvon, D.: Measurement of electron-phonon decoupling time in neutron-transmutation doped germanium at 20 mK. *J. Low Temp. Phys.* **93**(3–4), 289–294 (1993)
65. Alessandrello, A., Brofferio, C., Camin, D.V., Cremonesi, O., Giuliani, A., Pavan, M., Pessina, G., Previtali, E.: Signal modelling for TeO_2 bolometric detectors. *J. Low Temp. Phys.* **93**(3–4), 207–212 (1993)
66. Stefanyi, P., Zammit, C., Rentzsch, R., Fozzoni, P., Saunders, J., Lea, M.: Development of a Si bolometer for dark matter detection. *Phys. B* **194**, 161–162 (1994)
67. Efros, A., Shklovskii, B.: *Electronic Properties of Doped Semiconductors*. Springer Series in Solid-State Sciences. Springer, Berlin (1984)

68. Marcenat, C.: Etudes calorimetrique sous champ magnetique des phases basses temperature des composes Kondo (1986)
69. Xu, Jc, Watson, C.H., Goodrich, R.G.: A method for measuring the specific heat of small samples. *Rev. Sci. Instrum.* **61**(2), 814–821 (1990)
70. Flachbart, K., Gabáni, S., Gloos, K., Meissner, M., Opel, M., Paderno, Y., Pavlík, V., Samuely, P., Schubert, E., Shitsevalova, N., Siemensmeyer, K., Szabó, P.: Low temperature properties and superconductivity of LuB_{12} . *J. Low Temp. Phys.* **140**(5–6), 339–353 (2005)
71. Pilla, S., Hamida, J., Sullivan, N.: A modified dual-slope method for heat capacity measurements of condensable gases. *Rev. Sci. Instrum.* **71**(10), 3841–3845 (2000)
72. Gmelin, E.: Classical temperature-modulated calorimetry: a review. *Thermoch. Acta* **305**, 1–26 (1997)
73. Castro, M., Puértolas, J.: Simple and accurate ac calorimeter for liquid crystals and solid samples. *J. Therm. Anal.* **41**(6), 1245–1252 (1994)
74. Corbino, O.M.: Specific heat. *Phys. Z.* **12**, 292 (1911)
75. Rosenthal, L.A.: Thermal response of bridgewires used in electro explosive devices. *Rev. Sci. Instrum.* **32**(9), 1033–1036 (1961)
76. Filippov, L.: Procedure of measuring liquid thermal activity. *Inzh.-Fiz. Zh.* **3**(7), 121–123 (1960)
77. Birge, N.O., Nagel, S.R.: Wide-frequency specific heat spectrometer. *Rev. Sci. Instrum.* **58**(8), 1464–1470 (1987)
78. Jeong, Y.H., Bae, D.J., Kwon, T.W., Moon, I.K.: Dynamic specific heat near the Curie point of Gd. *J. Appl. Phys.* **70**(10), 6166–6168 (1991)
79. Moon, I.K., Jeong, Y.H., Kwun, S.I.: The 3ω technique for measuring dynamic specific heat and thermal conductivity of a liquid or solid. *Rev. Sci. Instrum.* **67**(1), 29–35 (1996)
80. Jewett, D.M.: Electrical heating with polyimide-insulated magnet wire. *Rev. Sci. Instrum.* **58**(10), 1964–1967 (1987)
81. Cahill, D.G.: Thermal conductivity measurement from 30 to 750 K: the 3ω method. *Rev. Sci. Instrum.* **61**(2), 802–808 (1990)
82. Handler, P., Mapother, D.E., Rayl, M.: AC measurement of the heat capacity of nickel near its critical point. *Phys. Rev. Lett.* **19**(7), 356–358 (1967)
83. Hatta, I.: History repeats itself: progress in ac calorimetry. *Thermochim. Acta* **300**(1), 7–13 (1997)
84. Pradhan, N., Duan, H., Liang, J., Iannacchione, G.: Specific heat and thermal conductivity measurements for anisotropic and random macroscopic composites of cobalt nanowires. *Nanotechnology* **19**(48), 485712 (2008)
85. Hashimoto, M., Tomioka, F., Umehara, I., Fujiwara, T., Hedo, M., Uwatoko, Y.: Heat capacity measurement of CePd_2Si_2 under high pressure. *Phys. B* **378**, 815–816 (2006)
86. Hemminger, W., Höhne, G.: Grundlagen der Kalorimetrie. Verlag Chemie, Weinheim (1979)
87. Sullivan, P.F., Seidel, G.: Steady-state, ac-temperature calorimetry. *Phys. Rev.* **173**(3), 679 (1968)
88. Maglic, K., Cezairliyan, A., Peletsky, V.: Compendium of Thermophysical Property Measurement Methods: Vol. 1, Survey of Measurement Techniques. Plenum Press, New York (1984)
89. Schilling, A., Jeandupeux, O.: High-accuracy differential thermal analysis: a tool for calorimetric investigations on small high-temperature-superconductor specimens. *Phys. Rev. B* **52**(13), 9714–9723 (1995)
90. Budaguan, B., Aivazov, A., Meytin, M., Sazonov, A.Y., Metselaar, J.: Relaxation processes and metastability in amorphous hydrogenated silicon investigated with differential scanning calorimetry. *Phys. B* **252**(3), 198–206 (1998)
91. Sturtevant, J.M.: Biochemical applications of differential scanning calorimetry. *Annu. Rev. Phys. Chem.* **38**(1), 463–488 (1987)

92. Rahm, U., Gmelin, E.: Low temperature micro-calorimetry by differential scanning. *J. Therm. Anal.* **38**(3), 335–344 (1992)
93. Junod, A.: An automated calorimeter for the temperature range 80–320 K without the use of a computer. *J. Phys. E: Sci. Instrum.* **12**(10), 945 (1979)
94. Junod, A., Bonjour, E., Calemczuk, R., Henry, J., Muller, J., Triscone, G., Vallier, J.: Specific heat of an $\text{YBa}_2\text{Cu}_3\text{O}_7$ single crystal in fields up to 20 T. *Physica C* **211**(3), 304–318 (1993)
95. Kharkovski, A., Binek, C., Kleemann, W.: Nonadiabatic heat-capacity measurements using a superconducting quantum interference device magnetometer. *Appl. Phys. Lett.* **77**(15), 2409–2411 (2000)
96. Graebner, J.: Modulated-bath calorimetry. *Rev. Sci. Instrum.* **60**(6), 1123–1128 (1989)
97. Lashley, J., Hundley, M., Migliori, A., Sarrao, J., Pagliuso, P., Darling, T., Jaime, M., Cooley, J., Hults, W., Morales, L.: Critical examination of heat capacity measurements made on a quantum design physical property measurement system. *Cryogenics* **43**(6), 369–378 (2003)
98. Newsome Jr, R., Park, S., Cheong, S.-W., Andrei, E.: Low-temperature measurements of the specific heat capacity of a thick ferroelectric copolymer film of vinylidene fluoride and trifluoroethylene. *Phys. Rev. B* **77**(9), 094103 (2008)
99. Javorský, P., Wastin, F., Colineau, E., Rebizant, J., Boulet, P., Stewart, G.: Low-temperature heat capacity measurements on encapsulated transuranium samples. *J. Nucl. Mater.* **344**(1), 50–55 (2005)
100. Preston-Thomas, H.: The international temperature scale of 1990(ITS-90). *Metrologia* **27**(1), 3–10 (1990)
101. Kennedy, C.A., Stancescu, M., Marriott, R.A., White, M.A.: Recommendations for accurate heat capacity measurements using a quantum design physical property measurement system. *Cryogenics* **47**(2), 107–112 (2007)
102. Giazotto, F., Heikkilä, T.T., Luukanen, A., Savin, A.M., Pekola, J.P.: Opportunities for mesoscopics in thermometry and refrigeration: physics and applications. *Rev. Mod. Phys.* **78**(1), 217 (2006)
103. Bachmann, R., Kirsch, H.C., Geballe, T.H.: Low temperature silicon thermometer and bolometer. *Rev. Sci. Instrum.* **41**(4), 547–549 (1970)
104. Doettinger-Zech, S., Uhl, M., Sisson, D., Kapitulnik, A.: Simple microcalorimeter for measuring microgram samples at low temperatures. *Rev. Sci. Instrum.* **72**(5), 2398–2406 (2001)
105. Schwall, R., Howard, R., Stewart, G.: Automated small sample calorimeter. *Rev. Sci. Instrum.* **46**(8), 1054–1059 (1975)
106. Stewart, G.R.: Measurement of low-temperature specific heat. *Rev. Sci. Instrum.* **54**(1), 1–11 (1983)
107. Bourgeois, O., Skipetrov, S., Ong, F., Chaussy, J.: Attojoule calorimetry of mesoscopic superconducting loops. *Phys. Rev. Lett.* **94**(5), 057007 (2005)
108. Riou, O., Gandit, P., Charalambous, M., Chaussy, J.: A very sensitive microcalorimetry technique for measuring specific heat of μg single crystals. *Rev. Sci. Instrum.* **68**(3), 1501–1509 (1997)
109. Fominaya, F., Fournier, T., Gandit, P., Chaussy, J.: Nanocalorimeter for high resolution measurements of low temperature heat capacities of thin films and single crystals. *Rev. Sci. Instrum.* **68**(11), 4191–4195 (1997)
110. Early, S., Hellman, F., Marshall, J., Geballe, T.: A silicon on sapphire thermometer for small sample low temperature calorimetry. *Physica B + C* **107**(1), 327–328 (1981)
111. Wilhelm, H., Lüthmann, T., Rus, T., Steglich, F.: A compensated heat-pulse calorimeter for low temperatures. *Rev. Sci. Instrum.* **75**(8), 2700–2705 (2004)
112. Tagliati, S., Rydh, A.: Absolute accuracy in membrane-based ac nanocalorimetry. *Thermochim. Acta* **522**(1), 66–71 (2011)
113. Tagliati, S., Rydh, A., Xie, R., Welp, U., Kwok, W.: Membrane-based calorimetry for studies of sub-microgram samples. *J. Phys.: Conf. Ser.* 052256 (2009) (IOP Publishing)

Thermal Properties of Solids at Room and Cryogenic
Temperatures

Ventura, G.; Perfetti, M.

2014, XI, 216 p. 104 illus., 3 illus. in color., Hardcover

ISBN: 978-94-017-8968-4